ORIGINAL RESEARCH

Nano-Encapsulated Taro Lectin Can Cross an in vitro Blood-Brain Barrier, Induce Apoptosis and Autophagy and Inhibit the Migration of Human U-87 MG Glioblastoma Cells

Raiane Vieira Cardoso[1], Patricia Ribeiro Pereira [1], Cyntia Silva Freitas[1], Anna Victoria De Freitas Silva[2], Victor Midlej [2], Carlos Adam Conte-Júnior [1], Vania Margaret Flosi Paschoalin [1]

[1]Departamento de Bioquímica, Universidade Federal do Rio de Janeiro, Rio de Janeiro, RJ, Brazil; [2]Instituto Oswaldo Cruz, Rio de Janeiro, RJ, Brazil

Correspondence: Vania Margaret Flosi Paschoalin, Av. Athos da Silveira Ramos 149 – sala 545 - Cidade Universitária - 21941-909, Rio de Janeiro, RJ, Brazil, Tel +55213938-7362, Fax +55213938-7266, Email paschv@iq.ufrj.br

Background: Tarin, purified from taro (*Colocasia esculenta*), promotes anticancer effect against glioblastoma cells, a heterogeneous and aggressive primary central nervous system tumor and one of the most challenging tumors for oncotherapy. If able to overcome the blood-brain barrier (BBB), tarin may comprise a natural defense against glioblastomas in a context of the development of novel drugs to control these malignant cell proliferations.

Methods: The anticancer effects of nano-encapsulated tarin were tested against U-87 MG cells and the molecular mechanisms involved in cell proliferation control were assessed by flow cytometry and transmission electron microscopy (TEM) analyses. The scratch assay was performed to investigate cell migration capacity, while nano-encapsulated tarin transport across the BBB was tested on the hCMEC/D3 endothelial cell line.

Results: Nano-encapsulated tarin induced autophagy in U-87 MG cells, characterized by the presence of autophagosomes as revealed by TEM and corroborating the flow cytometry analysis employing acridine orange. Additional ultrastructural changes, such as mitochondrial swelling, were also observed. The presence of apoptotic cells and caspase 3/7 activation indicate that nano-encapsulated tarin may also induce cell death through apoptosis. Glioblastoma cell proliferation was arrested in the G2/M cell cycle phase, and cell migration was delayed. Reduced cell proliferation and glioblastoma cell migration inhibition were significant, as tarin was efficiently transported across the BBB during in vitro assays.

Conclusion: Nano-encapsulated tarin may be effectively employed to inhibit glioblastoma cell proliferation and migration, as this novel formulation can overcome the BBB and induces carcinoma cell apoptosis and autophagy. Furthermore, nano-encapsulated tarin may comprise a novel chemotherapeutic agent against different tumoral lines, as it is able to control glioblastoma tumor proliferation by the same molecular mechanisms previously reported for breast adenocarcinomas. Additional studies should be carried out to clarify if nano-encapsulated tarin has a general effect on distinct carcinoma lines.

Keywords: *Colocasia esculenta*, GNA-related lectin, cell cycle arrest, caspase 3-7 activation, antitumoral lectin, transendothelial permeability

Introduction

Glioblastoma (GBM), a tumor arising from glial cells in the central nervous system (CNS), brain or spinal cord, is very aggressive, grows quickly and can invade and destroy surrounded healthy tissues. Glioblastoma prognoses comprise an average survival rate from 12 to 15 months. This prevalent and malignant brain tumor contains self-renewing, tumorigenic cancer stem cells that contribute to chemoresistance, heterogeneity (referring to the fact that different regions within a single glioblastoma tumor can present different molecular and genetic profiles) and infiltrative patterns,

Graphical Abstract
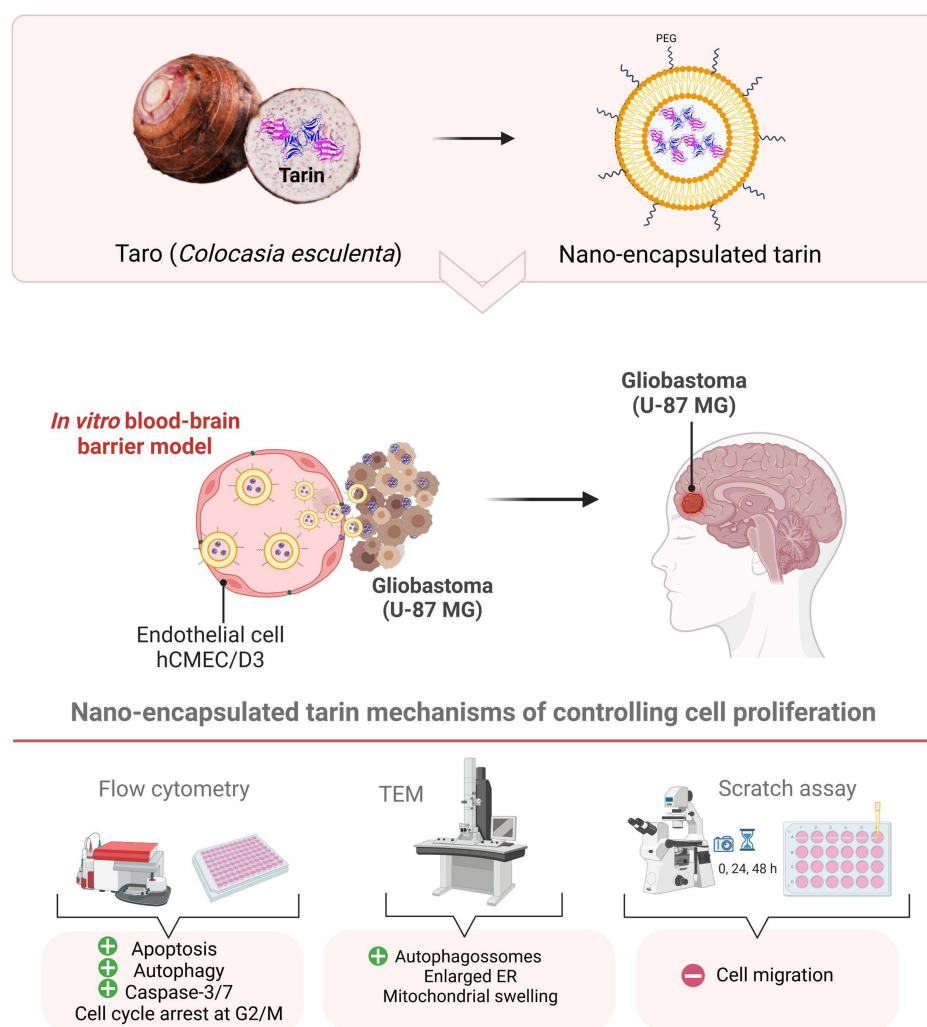
making complete tumor resection very difficult.[1–4] The molecular biology underlying glioblastomas is characterized by an intricate network of biochemical processes, highlighting the pressing need for developing targeted therapeutic approaches to overcome tumoral proliferation control challenges. In this context, the dysfunction of multiple molecular signaling pathways, including the epidermal growth factor receptor (EGFR)/AKT/phosphatase and tensin homolog (PTEN), protein kinase C (PKC), tumor suppressor protein p53 (P53), retinoblastoma protein (pRB), and vascular endothelial growth factor (VEGF) pathways, among others, are significant glioblastoma pathogenesis aspects. The interaction of these mechanisms amplified by the blood-brain barrier (BBB), which restricts access of chemotherapy agents to the tumor core, and cancer stem-like cells, recognized for their intrinsic resistance to chemotherapy and radiotherapy, are very challenging to overcome, and, may contribute significantly to malignant glioblastoma progression and recurrence.[5–10]

Glioblastoma treatments are one of the most challenging oncology therapeutics, as this tumor is considered mostly incurable, with no available treatment to slow its growth or reduce symptoms. The current therapeutic regimens for this tumor include surgery for tumoral tissue removal, although its invasive characteristics make surgery resection very difficult. Glioblastoma is also resistant to radiotherapy, and despite the different ways of administering chemotherapeutic

drugs glioblastoma locations beyond the BBB limit drug penetration and effectiveness, making these tumors resistant to these treatments.[11–16] Currently the first-line chemotherapy drug for glioblastoma is temozolomide (TMZ), a monofunctional alkylating agent whose therapeutic efficacy is far from optimal, as it is highly toxic and has difficulty in penetrating the BBB.[17–19] TMZ resistance is noted due to several molecular mechanisms, including DNA repair, multidrug transporters, epigenetic modifications, microRNAs, extracellular vesicles, and autophagy.[20]

Innovative therapeutic interventions for glioblastoma proliferation control have emerged, in addition to conventional chemotherapy and radiotherapy, such as carmustine wafers (Gliadel®),[21,22] which consists in local chemotherapy, of low-intensity alternating electric fields (Optune® therapy), implanted directly into the intracranial tissue.[23–26] To effectively bypass the BBB and deliver compounds specifically targeting glioblastoma cells, a promising class of nanocarrier, liposomes, has been considered for glioblastoma therapy, as the lipophilic nature of this molecules facilitates the penetration of both hydrophilic- and hydrophobic-loaded drugs across the BBB, delivering them directly to glioblastoma cells. The inclusion of polyethylene glycol (PEG) in nanoliposome formulations gives these molecules the ability to easily cross the endothelial barrier and accumulate in tumoral tissues, making this the best choice of active antitumorigenic agent. Additionally, pegylated nanoliposomes offer a considerable advantage by avoiding their recognition by macrophages, slowing their bloodstream clearance and prolonging the stay of this pharmacological agent in the bloodstream, minimizing pharmacological compound losses over time.[27,28] Numerous studies have been carried out aiming at the formulation of liposomal delivery systems for cancer therapy since the approval of the first liposome formulation for passively targeting carcinoma cells occurred in early 1995,[28] with some of them already being employed in clinical glioblastoma treatment trials. Studies have focused not only on the use of nano-encapsulating therapeutic agents, but also on their ability to specifically target the tumoral cells. In this sense, the Doxil®, Myocet®, Depocyt®, NL CPT-11 (Phase I trial),[29,30] 2B3-101 (phase I/II - NCT01386580) and C225-ILs-Dox (phase I - NCT03603379) formulations are evaluated for glioblastoma chemotherapy.[31,32]

Natural products have been shown to influence multiple oncogenic signaling pathways simultaneously by modulating the activity or expression of their molecular targets. They generate intracellular signals that inhibit cell proliferation by arresting of the cell cycle and trigger events that lead to cancer cell death, such as apoptosis. Natural products can both inhibit migration/invasion, and difficult angiogenesis. Natural chemotherapy substances can be used in cases where cancer is resistant to conventional treatment. Furthermore, the high costs of conventional chemotherapy drugs and the increasing incidence of cancer have challenged researchers to research more cost-effective and environmentally friendly alternatives. In this context, natural products are highly advantageous, due to their chemical diversity, low toxicity, safety, and availability, making them an attractive and affordable alternative to synthetic products.[33,34] One approach to improve the delivery of natural substances is the use of drug nano carriers, which provide protection to the transported substances while also offering the potential for increased drug concentrations at target sites. One of the most extensively studied and widely employed compound in drug delivery systems comprises liposomes, spherical structures whose wall is formed by a bilayer of amphiphilic phospholipids surrounding an aqueous core.[28,35]

Tarin, a member of the GNA-lectin family, is a four-subunit hetero-tetrameric 47 kDa protein purified to over 90% purity obtained from taro (*Colocasia esculenta* L. Schott).[36,37] Its crystallographic structure has been determined[38] and it displays antitumorigenic and immune-modulatory activities, as demonstrated previously by our research group.[36,39–42] Tarin also exhibits an expanded binding site for complex mannose-rich N-glycan chains - 49, 212, 213, 358, 465, and 477- found on the surface of antigens, displays recognized biocidal activities against viruses and insects.[36–41,43–45] Previous studies employing microarray analyses have revealed that tarin reversibly interacts with specific high mannose and complex N-glycans found in glycoproteins and glycolipids present in cancerous cells, including paucimannose and their corresponding fucosylated forms, found in U-87 MG cells, thus proposing tarin as a GBM biomarker.[37,46] These plant lectin family members also bind to tumor glycan cells and promote cell death by modulating apoptotic and autophagic signaling pathways.[42,47–49] These findings encouraged us to investigate the anticancer activity of tarin when nano-encapsulated in pegylated liposomes. This novel formulation exhibits a nano size of 150 nm and can release tarin in a controlled manner at pH conditions ranging from 4.6 to 7.4, found in various physiological environments, allowing it to probably be able to overcome the BBB, a significant hurdle in treating central nervous system tumors and exerting its effects.[40,45]

We have previously demonstrated that nano-encapsulated tarin exhibits promising anticancer properties against human mammary adenocarcinoma (MDA-MB-231) and glioblastoma U-87 MG cells, explained by the aforementioned eclectic tarin-carbohydrate interaction.[37,40,45] The anticancer mechanisms of both cell lines have been investigated in parallel. The anticancer efficacy of nano-encapsulated tarin against MDA-MB-231 includes apoptosis induction, with caspase-3/7 activation, cell cycle arrest at G0/G1, cell migration inhibition and the promotion of ultra-structural alterations compatible with autophagy-dependent cell death.[42] Herein, we report the anticancer mechanisms triggered by tarin loaded in nanoliposomes against U-87 MG, following a similar methodology to elucidate if tarin exhibits a common pattern model of action and if it can cross an in vitro BBB. The convergence of findings indicates that tarin may not only inhibit GBM proliferation and migration but also potentially act as a natural chemotherapeutic molecule against other carcinoma types, as already demonstrated for human mammary adenocarcinoma, suggesting a broader relevance of our research. This could position nano-encapsulated tarin as a versatile candidate for the development of novel chemotherapeutic drugs.

Materials and Methods
Tarin Purification
Colocasia esculenta (L). Schott corms were purchased at a local market in Rio de Janeiro, Brazil, and a voucher specimen of a taro plant was deposited (RFA-39.962) at the RFA Herbarium (https://specieslink.net/col/RFA) belonging to the Biology Institute's Botany Department at the Federal University of Rio de Janeiro (Rio de Janeiro, RJ, Brazil). A crude taro extract was prepared as previously described[50] and purified through affinity chromatography by fast-performance liquid chromatography (FPLC) to over 90% homogeneity, employing an Akta purifier 10 (GE Healthcare, IL, USA) coupled to a 3GA Cibacron Blue column (Sigma-Aldrich Co, MO, USA).[36] The tarin fraction was freeze-dried (Liobras, SP, BRA), and protein concentrations were estimated using the Total Protein Kit, Micro Lowry, Peterson's Modification employing bovine serum albumin (BSA) (Sigma-Aldrich Co) as the external standard.

Tarin-Loaded Nanoliposome Preparation
Liposomes about 150 nm in size and with a polidispersity index (PdI) of 0.168 ± 0.03 evaluated by dynamic light scattering (DLS) (Zetasizer Malvern Panalytical, Almelo, NLD) were prepared according to the methodology described in our previous study.[39] DOPE (1,2-dioleoyl-sn-glycerol-3-phosphoethanolamine); MPEG 2000-DSPE 1.2-distearoyl-sn-glycer-3-phosphoethanolamine-N-[amino (polyethylene glycol)-2000] (Lipoid GMBH) and cholesteryl hemisuccinate (CHEMS) (Sigma-Aldrich Co) were dissolved in chloroform, comprising the solvent resulting in the best lipid film solubilization, according to our previous study.[39] After removing the organic solvent using a rotary evaporator (Buchi, SP, BRA), the resulting thin lipid film was rehydrated in 0.3 M ammonium sulfate pH 7.4, containing 1 mg/mL tarin.[39] The tarin-loaded nanoliposomes were then collected by ultracentrifugation at $150,000 \times g$ for 90 min at 4 °C (Beckman Coulter, IN, USA). Nano-encapsulation efficiency was determined by quantifying non-encapsulated tarin in the supernatant using the Total Protein Kit. Protein quantification as carried out according to the Peterson methodology, the most suited for lipid-rich samples. Sample blanks and controls were prepared in the same way, to avoid interference.

Human Cell Lines and Culture Conditions
Human U-87 MG glioblastoma cells (ATCC HTB-14) and human brain hCMEC/D3 line microvessels (BCRJ code 0401) were obtained from the Rio de Janeiro Cell Bank (BCRJ, RJ, BRA), available at https://bcrj.org.br/.

The U-87 MG cells were seeded at 1.0×10^6 cells/mL in a DMEM high glucose Dulbecco medium supplemented with 10% fetal bovine serum (FBS) (Gibco Life Technologies, NY, USA). Cells were incubated at 37 °C in a humidified atmosphere containing 5% CO_2 in 75 cm² culture flasks until reaching a semi-confluent layer and trypsinized with the TrypLE™ express enzyme (Gibco Life Technologies) for 5 min at 37 °C followed by centrifugation at $200 \times g$ for 10 min, transfer to 24-well plates at a density of 1.0×10^5 cells per well and culturing for an additional 24 h. The culture medium was then replaced by a fresh one containing free or nano-encapsulated tarin (160 μg/mL), or the equivalent volume of empty liposomes, etoposide (2 μM), TMZ (33 μg/mL), or cytochalasin (5 μM) (Thermo Fisher Scientific, MA,

USA) and incubated for 24 h and 48 h. The cells were then used to investigate cell migration capacity through the scratch assay, assess ultrastructural morphology tumor cell changes by transmission electron microscopy (TEM), elucidate cell death mechanisms through autophagy and apoptosis assessments, and evaluate caspase activation and cell cycle changes employing flow cytometry. The ability of nano-encapsulated tarin to cross the BBB was investigated through the BBB assay, as described in the following sections.

The hCMEC/D3 cells used in the BBB assays were seeded at 1.0×10^6 cells/mL in EBM-2 medium (Lonza, BS, CHE) supplemented with 5% FBS, chemically defined, lipid concentrated (diluted at 1/100), 5 µg/mL ascorbic acid, 1 ng/mL fibroblast growth factor (bFGF), HEPES 10 mm and 1.4 µM hydrocortisone. Before seeding, 75 cm^2 culture flasks were pre-coated with 0.1 mg/mL type I rat tail collagen (Thermo Fisher Scientific, MA) for 1 h at 37 °C. The cells were then added and incubated at 37 °C in a humidified atmosphere containing 5% CO_2 until reaching a semi-confluent layer. These cells were used to perform the BBB assay in 24-transwell plates.

In vitro Transport of Nano-Encapsulated Tarin Across the BBB Model

The hCMEC/D3 cells were seeded on transwell filters (0.4 µm pore size) pre-coated with type I collagen (Thermo Fisher Scientific) in 24-well plates at a density of 5.0×10^4 cells/cm^2 using supplemented EBM-2 medium (Lonza). The transport assay was carried out for twelve days after seeding, with medium replacement every four days. During this period, the cell monolayer was inspected under a microscope and transendothelial electrical resistance (TEER) was monitored with a Millicell ERS-2 Epithelial Volt-Ohm meter (Millipore, MA, USA). Simvastatin (1 nM) (Sigma-Aldrich Co) was added to the supplemented EBM-2 medium 24 h prior to the beginning of the transport assay. Monolayer permeability was tested using 20 µM of lucifer yellow (Sigma-Aldrich Co). After complete monolayer formation (12 days), the nano-encapsulated tarin (160 µg/mL) or an equivalent volume of empty liposomes were added to the upper chamber containing 20 µM of lucifer yellow, and permeabilities were calculated.[51] The plates were incubated under standard conditions (5% CO_2 and 37 °C), at predetermined times of 60, 120 or 180 min, and 100 µL aliquots were collected from the bottom chamber and analyzed using a Victor™ X microplate reader (PerkinElmer Inc., MA, USA) at an excitation wavelength of 430 nm and emission wavelength of 535 nm for lucifer yellow detection. The nano-encapsulated tarin was monitored employing a UV-Vis spectrophotometer (Shimadzu, JPN) at 300 nm.

Nano-Encapsulated Tarin-Treated U-87 MG Cell Migration Patterns

Cell migration was assessed through the wound healing assay.[52] After reaching a semi-confluent layer in the 24-well plates, a linear scratch was performed using a sterile 200 µL-pipette tip followed by careful cell washing with phosphate-buffered saline (PBS) at pH 7.4. Subsequently, a serum-free DMEM High Glucose medium containing 40, 80, 160 µg/mL of free or nano-encapsulated tarin or the equivalent volume of empty liposomes, were added to the wells. The concentrations employed in the present study are based on previous studies that determined the antitumoral IC_{50} of nano-encapsulated tarin against U-87 MG cells.[40] TMZ (33 µg/mL), or cytochalasin D (5 µM), or the culture medium alone was added to the wells. Cell migration in every well was monitored under an inverted optical microscope (Biofocus, MG, BRA) for 24 h and 48 h. The cell-free area after each treatment and time period was estimated using the Image J software, available at https://imagej.nih.gov/ij/download.html) (National Institutes of Health – NIH, MD, USA) and compared to the initial area.

Morphological Analysis of U-87 MG Subcellular Structures Following Exposure to Nano-Encapsulated Tarin

The ultrastructural morphology of U-87 MG cells treated with free tarin (160 µg/mL), nano-encapsulated tarin (160 µg/mL), or the equivalent volume of empty liposomes for 24 h and 48 h, were examined by TEM, as described previously.[53] Treated cells were fixed with 2.5% glutaraldehyde in a 0.1 M sodium cacodylate buffer pH 7.4 for 1 h at room temperature, post-fixed in a 1% osmium tetroxide (Sigma-Aldrich Co) and 0.8% potassium ferrocyanide solution and dehydrated with increasing acetone concentrations of 70%, 90%, and 100% (Sigma-Aldrich Co), embedded in Epon resin

and polymerized at 60 °C. Ultrathin sections (60–70 nm thickness) were stained with 5% uranyl acetate (EMS) and lead citrate and the micrographs were recorded employing an HT7800 RuliTEM microscope (Hitachi, TKY, JPN).

Investigation of U-87 MG Cell Death Mechanisms - Apoptosis and Autophagy - Upon Treatment by Nano-Encapsulated Tarin

Cell apoptosis was assessed by using Annexin V FITC/propidium iodide (PI) Apoptosis Kit (Thermo Fisher Scientific), according to the manufacturer's instructions. Following treatment, U-87 MG cells were harvested from 24-well plates by trypsinization followed by centrifugation at 200 × g for 10 min and washed twice with ice-cold PBS at pH 7.4. Cells were then resuspended in 100 μL of Annexin V binding buffer containing 5 μL of FITC Annexin V and 1 μL of 100 μg/mL propidium iodide (PI), incubated in the dark for 15 min at room temperature and analyzed employing a BD Accuri C6 flow cytometer (BD Bioscience, NJ, USA) using the FL-1 and FL-3 channels, for Annexin V-FITC and PI, respectively. Results were expressed as the percentage of viable cells and/or early apoptotic, late apoptotic, dead/necrotic cells.

Acidic autophagic vacuoles in U-87 MG cells were investigated through acridine orange staining, which glows green in unaffected cellular compartments and red in acidic ones, such as the mature/late autophagosomes.[54] Briefly, U-87 MG cells were harvested from the 24-well plates by trypsinization, followed by centrifugation at 200 × g for 10 min, washing with PBS pH 7.4 and treatment t with acridine orange at 1 μg/mL (Sigma-Aldrich Co) for 15 min at room temperature in the dark. Stained cells were analyzed on an Accuri C6 BD plus flow cytometer (BD Bioscience, NJ, USA) using the FL-1 and FL-3 channels to detect red and green fluorescence, respectively, and the results were expressed as R/GFIR ratio intensities.

Activation of Caspase-3 and Caspase-7 in U-87 MG Cells Exposed to Nano-Encapsulated Tarin

The green Caspase-3/7 Detection Kit™ (Thermo Fisher Scientific) following the manufacturer's instructions was used to investigate caspase-3 and caspase-7 activation. The U-87 MG cells treated by nano-encapsulated tarin (160 μg/mL) were harvested from the 24-well plates and washed, as described previously. The cell pellets were resuspended in 250 μL of the caspase-3/7 detection reagent and incubated at 37 °C for 30 min in the dark and analyzed by flow cytometry using the same apparatus as reported previously, on the FL-1 channel.

Nano-Encapsulated Tarin-Treated U-87 MG Cell Cycle Analysis

The U-87 MG cells harvested from the 24-well plates by trypsinization were centrifuged at 200 × g for 10 min, and resuspended in cold 70% ethanol, followed by overnight incubation at −20 °C. After ethanol removal by centrifugation at 800 × g for 5 min., the cell pellets were resuspended in PBS containing propidium iodide (50 μg/mL), Triton X-100 (0.1%, v/v) and RNase-free DNase (1 μg/mL) for 1 h at 37 °C.[55] The cell cycle profiles (G0/G1, S, and G2/M) were then determined using the BD Accuri C6 plus software.

Statistical Analysis

All experiments were performed in triplicate and the results were expressed as the means and standard deviations. Data were compared by a one-way or two-way Analysis of Variance (ANOVA) followed by multiple comparisons using the Tukey's post-hoc test or the multiple *t*-test followed by the Holm-Sidak method post-test. The GraphPad Prism version 7 software (GraphPad, CA, USA) was used for all statistical analyses, considering $p < 0.05$ as significant.

Results and Discussion
Nano-Encapsulated Tarin Inhibits U-87 MG Cell Migration

Nano-encapsulated tarin at 160 μg/mL inhibited the migration of human U-87 MG glioblastoma cells early after the first 24 h of treatment, with the effects lasting up to 48 h (Figure 1A–D). The nano-encapsulated tarin was not, however, effective in inhibiting glioblastoma cell migration at lower concentrations (40 μg/mL or 60 μg/mL) (Figures 1B and C, S1 and S2). As expected, TMZ at 33 μg/mL and cytochalasin D at 5 μM completely inhibited U-87 MG cell migration
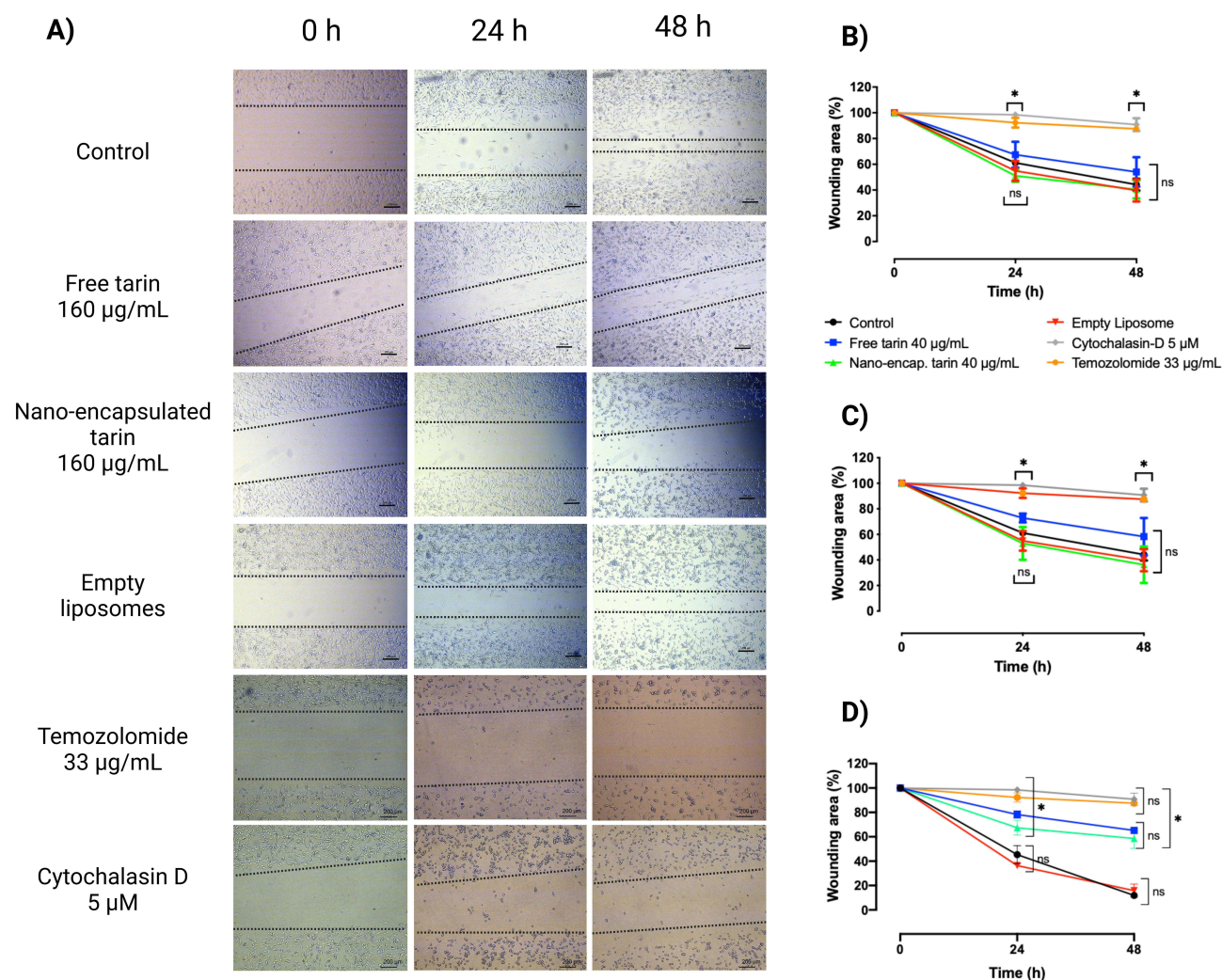
Figure 1 U-87 MG migration following nano-encapsulated tarin treatment over 48 h. (**A**). Representative photomicrography of the scratch assay depicting U-87 MG cells migration patterns at 0 h, 24 h and 48 h after treatment with nano-encapsulated tarin (160 µg/mL), free tarin (160 µg/mL) or the equivalent volume of empty liposomes, TMZ (33 µg/mL) or cytochalasin D (5 µM). (**B**) Wound area percentages over time and after challenging the cells with nano-encapsulated tarin at 40 µg/mL, (**C**) 80 µg/mL and (**D**) 160 µg/mL. Wound area was calculated using the ImageJ software and considering the initial (0 h) wound area as 100%. Data are presented as means ± SD. *p <0.05, ns- not significant. Scale bars indicate 200 nm.

(Figure 1B–D). Free tarin at 160 µg/mL promoted a similar inhibitory effect on U-87 MG migration compared to nano-encapsulated tarin (Figure 1A–D). In contrast, the empty liposomes had no effect on cell migration at all doses, like the control group, evidencing no encapsulating agent interference on cell migration inhibition (Figure 1A–D).

Cytochalasin D binds with high affinity to the growing ends of actin filament cores (F-actin), inhibiting both the polymerization and depolymerization of its subunits and consequently affecting numerous cellular activities including cell migration, explaining the observed cell inability to migrate to wounding area.[56,57] TMZ is a first-line drug with proven efficacy against glioblastomas, with previously reported effectiveness in inhibiting cell growth and glial cell migration.[58–60] Altogether, cytochalasin D, TMZ and nano-encapsulated tarin exerted inhibitory migration effects and promoted morphological changes in U-87 MG cells.

Cell migration is one the initial cancer metastasis stages, imputing a putative role to tarin in controlling U-87 MG cell metastasis.[61–63] Moreover, nano-encapsulated tarin was shown to be non-cytotoxic to healthy human fibroblast cell lines (HFF-1) at 160 µg/mL. Cells were not affected at concentrations ranging from 106.62 µg/mL to 217.5 µg/mL after 24 and 48 h of exposure.[40,42] These results reinforce that the effective tarin concentration can be safely used to control GBM cells.

Autophagosomes Formation in U-87 MG Cells Challenged with Nano-Encapsulated Tarin

The U-87 MG cell morphology from TEM analyses revealed the presence of autophagic vacuoles after 24 h of exposure to nano-encapsulated or free tarin, both at 160 μg/mL. Cytoplasmic structures, such as mitochondria, delimited by endoplasmic reticulum (ER) membranes were observed (Figure 2e–h). Besides autophagosome formation after 48 h of treatment, multivesicular bodies were also routinely observed in U-87 MG cells (Figure 2e–h). Mitochondrial swelling was also detected in cells treated with nano-encapsulated tarin at 24 h and 48 h, and observed later, after 48 h of exposure, in free tarin-treated cells (Figure 2g and h). Both cells treated with empty liposomes and untreated cells exhibited well-preserved mitochondria and nucleus, similar to other subcellular structures (Figure 2a–d), corroborating findings described in previous migration assays, reinforcing the non-toxic nature of the nano-liposomes used as encapsulating agents to load tarin.

Mitochondrial swelling has been associated with ER stress in Huh-7 cells treated with curcumin, a phenolic compound with well-established antioxidant properties.[64,65] Similarly, as reported for other bioactive compounds, stress conditions cause calcium release by the ER, which is rapidly absorbed by mitochondria through the mitochondrial calcium uniporter, resulting in mitochondrial swelling. This increased mitochondrial calcium opens permeability transition pores (PTP), leading to the release of cytochrome c from the mitochondrial membrane and subsequent caspase pathway activation, culminating in cell death.[64,66,67]
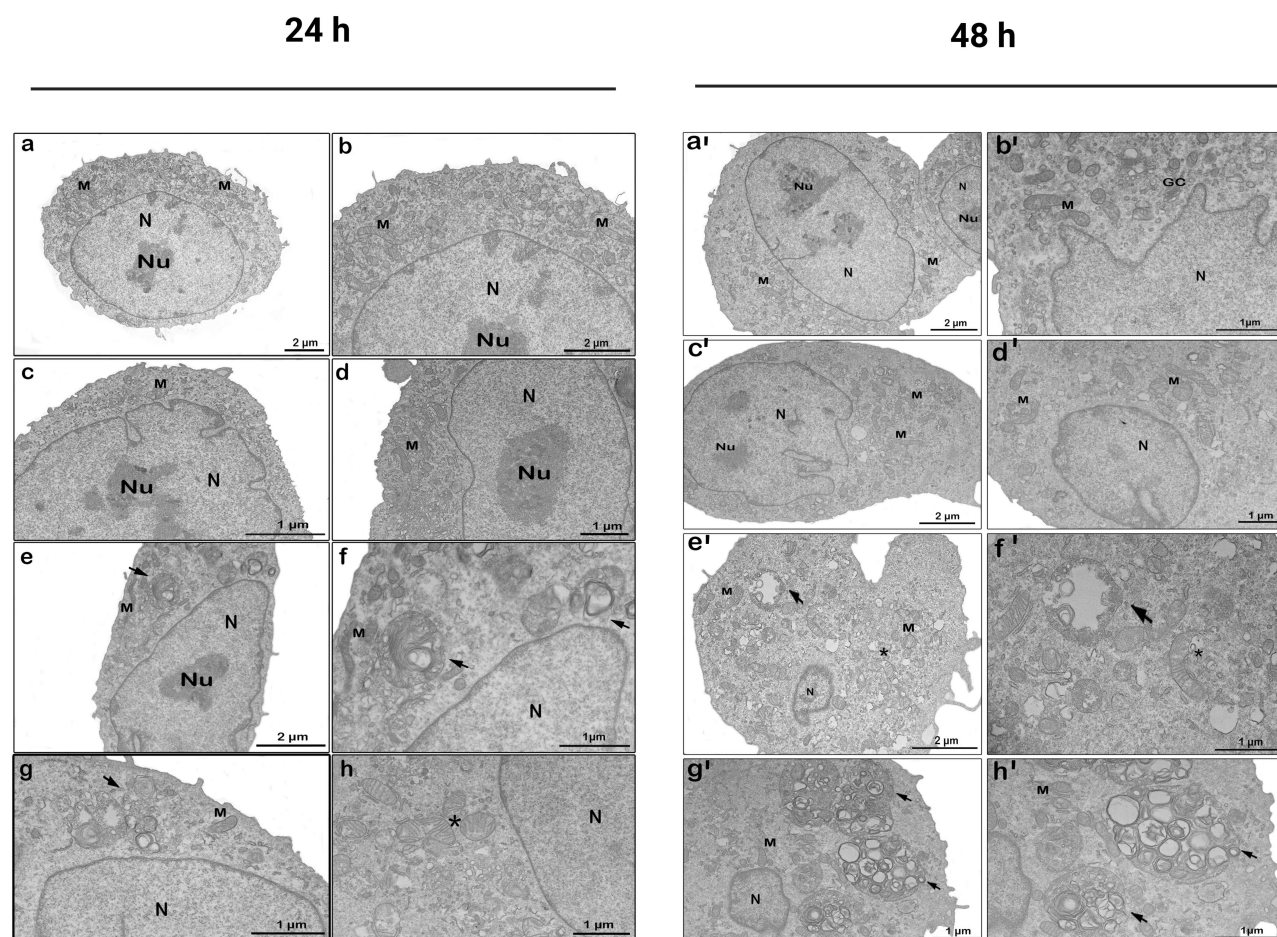

Figure 2 Ultrastructure of U-87 MG cells treated with nano-encapsulated tarin at 160 μg/mL for up to 48 h evaluated by transmission electron microscopy. Untreated U-87 MG cells (a - b, a' - b'), cells treated with empty liposomes (c – d, c' – d'), cells treated with free tarin (160 μg/mL) (e – f, e' – f'); cells treated with nano-encapsulated tarin (160 μg/mL) (g – h, g' – h'). Arrows indicate autophagosome formation and multivesicular bodies, *marks mitochondria swelling.
Abbreviations: N - nucleus, Nu - nucleolus; M - mitochondria, GC - Golgi Complex.
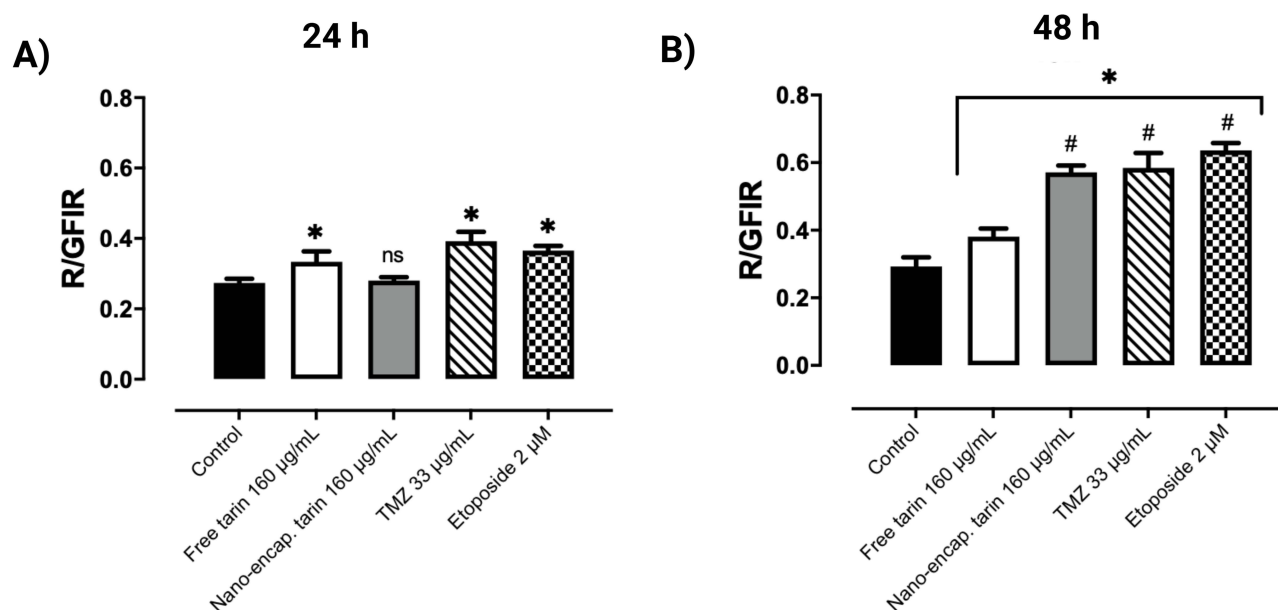
Figure 3 Autophagy induced by free or nano-encapsulated tarin. U-87 MG cells were treated with free or nano-encapsulated tarin (160 μg/mL), TMZ (33 μg/mL), or etoposide (2 μM) for 24 h (**A**) or 48 h (**B**). Cells were stained with acridine Orange to reveal acidic vacuolar organelles (AVOs) and data were expressed as the green/red fluorescence intensity ratio (R/GFIR). All experiments were performed in triplicate, where *represents a significant difference compared to the control group, and # in comparison to the same group at 24 h, considering p < 0.05.
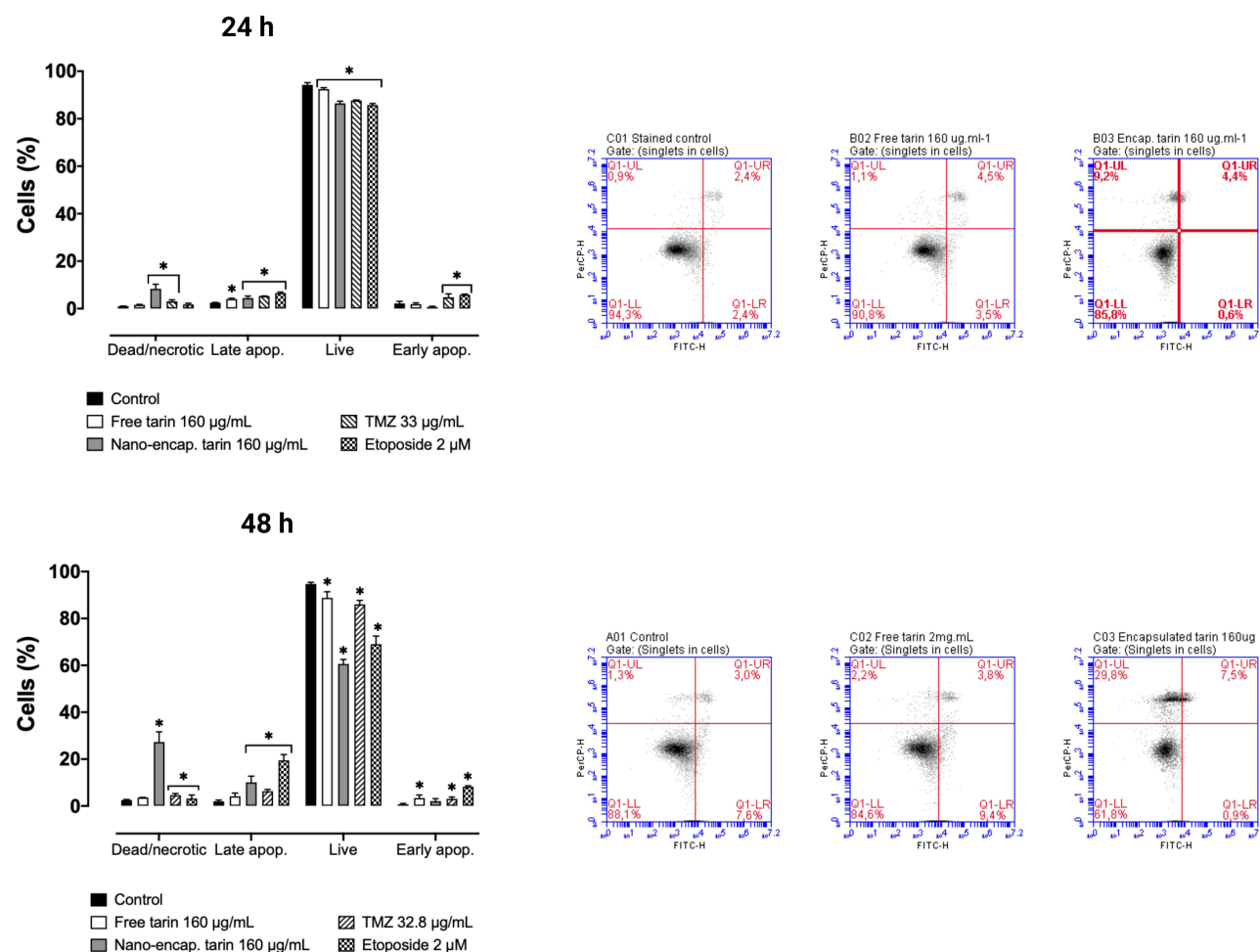
Autophagy induction enhances the number of acidic vacuolar organelles (AVOs) due to an increase in autolysosomes, estimated by increasing R/GFIR ratios, indicating higher red fluorescence compared to the green fluorescence of acridine orange.[54] Autophagosome formation induced by tarin in both its free or nano-encapsulated forms was corroborated by acridine orange treated glioblastoma cell staining and AVOs estimations through R/GFIR ratios (Figure 3A and B). After 48 h of exposure to nano-encapsulated tarin at 160 μg/mL, the treated U-87 MG cells exhibited high numbers of AVOs, comparable to those triggered by TMZ or etoposide (Figure 3B), while no effect was observed at 24 h (Figure 3A). On the other hand, a significant AVOs increase was detected early in the 24 h-exposure of U-87 MG to free tarin at 160 μg/mL, persisting for up to 48 h (Figure 3A and B).

The presence of autophagosomes is characteristic of the cell autophagy process, which can be triggered by tarin as a mechanism to escape cell death and may also contribute to apoptosis. GNA-related lectins usually cause cancer cell autophagy effects, like noted for various antitumoral drugs, as an anti-tumorigenic cell death mechanism. In these cases, cell death may either occur jointly by both autophagy and apoptosis activation, or apoptosis may be caused by autophagy only. Although autophagy can be considered a survival mechanism inhibiting cell death, when excessive, irreversibly culminates in cell death.[28,68–73] Thus, although autophagy can comprise a therapeutic target during cancer treatment as a cytoprotective mechanism, it can also be considered a therapy-induced signal to trigger tumor cell death.[74,75]

Apoptosis and Caspase 3/7 Activation in U-87-MG Cells Challenged with Tarin-Loaded Nanoliposomes

To assess whether exposure to nano-encapsulated tarin at 160 μg/mL would induce cell death by apoptosis, a double labeling with Annexin V-FITC and PI was performed, and flow cytometry analyses were conducted after 24 h and 48 h (Figure 4).

Late apoptotic cells were detected in U-87 MG cultures after 24 h-exposure to both free or nano-encapsulated tarin followed by a decrease (14.2%) in viable cells (Figure 4, upper panel). An increase (9.2%) in dead/necrotic cells was also observed in U-87 MG cultures treated with nano-encapsulated tarin (Figure 4, upper panel). This outcome increased (29.8%) after 48 h of exposure, when higher percentages of dead/necrotic and late apoptotic cells were observed (Figure 4, bottom panel), indicating a prolonged and sustained nano-encapsulated tarin treatment effect. On the other

Figure 4 Apoptosis assessment in U-87 MG cells challenged with nano-encapsulated tarin. U-87 MG cells exposed to free or nano-encapsulated tarin at 160 μg/mL, TMZ (33 μg/mL) or etoposide (2 μM) for 24 h and 48 h treatments. Percentages of dead/necrotic, early or late apoptotic and live cells were estimated by flow cytometry analyses following annexin V-FITC and PI staining. Percentages are displayed in the left panel while representative dot-plots are shown in the right panel. Quadrant plots display necrotic cells in Q1-UL, late apoptotic cells in Q1-UR, live cells at Q1-LL and early apoptotic cells in Q1-LR.* Indicates significant results compared to control cells, considering p <0.05.

hand, free tarin triggered a slight increase in late apoptotic cells after 24 h (4.5%) and in early apoptotic cells at 48 h (9.4%) (Figure 4). The free tarin form promoted a lower extension rate effect, which suggests that prolonged and sustained nano-liposome delivery to the intracellular media can boost tarin intensity and duration effects. Further experiments, such as the uptake assay, should be conducted to clarify the endocytosis mechanism responsible for internalizing and releasing tarin from nanoliposomes. Proteomic analyses are in progress and should also help identify proteins and/or peptides involved in endocytic mechanisms, as well as in anti-tumoral mechanisms activated upon treatment by nano-encapsulated tarin.

To evaluate caspase 3 and 7 activation, U-87 MG cells treated with free or nano-encapsulated tarin,TMZ or etoposide were labelled with DEVD, a four-amino acid peptide conjugated to a nucleic acid-binding dye, to investigate apoptosis activation (Figure 5). An increase in the percentage of cells harboring activated caspase 3/7 was observed after 24 h cell exposure to nano-encapsulated tarin at 160 μg/mL. No activation was observed after treatments with free tarin, etoposide or TMZ (Figure 5, upper panel). On the other hand, after 48 h, nano-encapsulated tarin boosted the effect, reinforcing the controlled and sustained release of tarin loads. An increase in caspase activation was also detected after treatment with TMZ or etoposide. Again, free tarin did not promote any detectable caspase 3/7 activation (Figure 5, bottom panel), corroborating the discrete observed increase in the amount of late and early apoptotic cells (Figure 4).
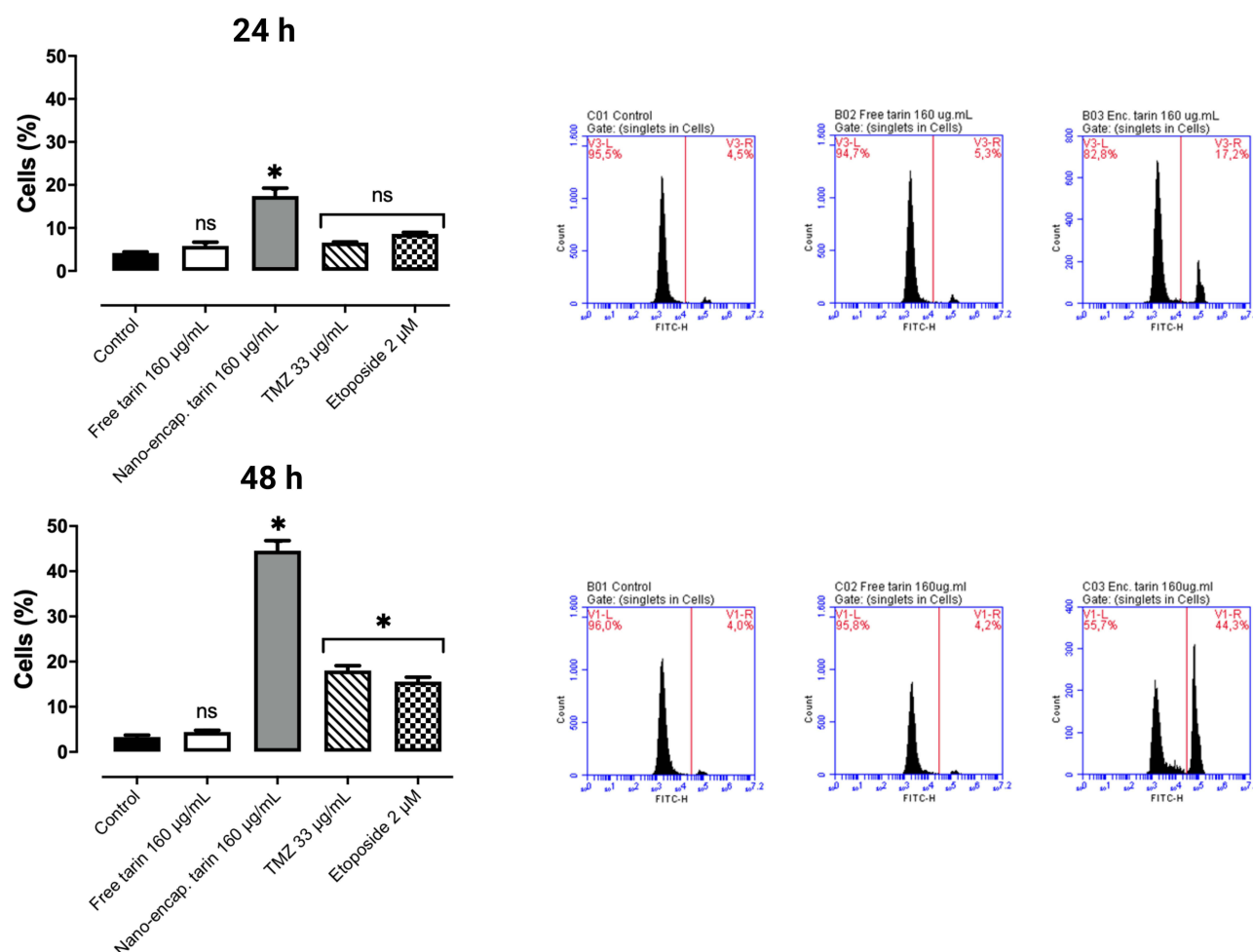
Figure 5 Caspase 3/7 activation in U-87 MG cells treated with nano-encapsulated tarin. U-87 MG cells were exposed to free and nano-encapsulated tarin (160 μg/mL), TMZ (33 μg/mL) or etoposide (2 μM) for 24 h and 48 h. The percentage of cells presenting caspases 3/7 activation was inferred using a fluorogenic tetrapeptide substrate (DEVD) conjugated to a nucleic acid-binding green dye (left panel). Histograms were obtained through a flow cytometer in the FL-1 channel (right panel). Experiments were performed in triplicate, where * represents significant differences compared to the control group with $p < 0.05$. ns – non-significant. Cells with non-activated caspases are on the VI-L side and those with activated caspases, on the VI-R side.

Altogether, the results reported herein suggests that exposure to nano-encapsulated tarin triggers mitochondrial swelling that, in turn, impairs mitochondria homeostasis, which might be caused by ER stress, as noted in the TEM results following tarin treatment (Figure 2). The ER stress may, in turn, lead to an influx of calcium ions to the cytoplasm, which triggers the release of cytochrome c and activates the caspase cascade.[64,76,77] Cytochrome c released from mitochondria into the cytosol binds to Apaf-1, the apoptotic protease activating factor 1, forming an apoptosome complex that, in turn, activates caspase 9, cleaving and activating caspase-3/7 and, finally, triggering apoptosis.[77] Once again, the results reported herein evidence that tarin release from nanocapsules takes place in a controlled manner, which should be considered a promising strategy for glioblastoma chemotherapy. Furthermore, nano-encapsulation may increase tarin half-life in the bloodstream, confer protection against proteases and avoid unspecific interactions, resulting in reduced tarin clearance and reinforcing its anticancer effect with no cytotoxicity.[78,79]

The U-87 MG Cell Cycle Is Affected by Exposure to Nano-Encapsulate Tarin

The treatment of U-87 MG cells by nanoencapsulated tarin promoted changes in cell cycle phases, perceived after the first 48 h by labelling the cells with PI (Figure 6). A significant increase in the percentage of cells in G2/M was noted following exposure to nano-encapsulated tarin in a similar way to etoposide, which is recognized cause of G2/M cell cycle arrest (Figure 6, bottom panel).[80,81] The increased number of cells in the G2/M phase was accompanied by
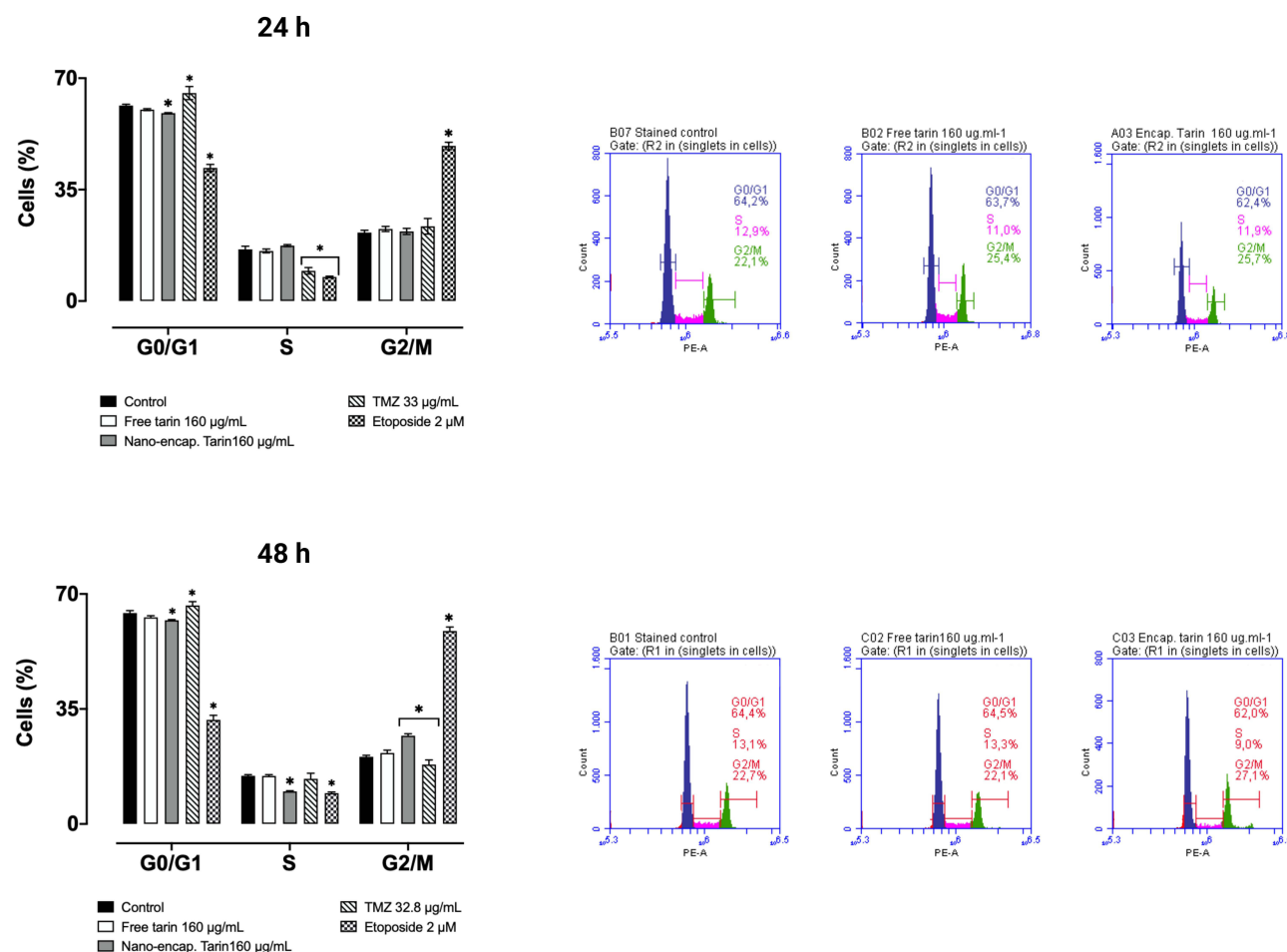
24 h

48 h

Figure 6 Effect of nano-encapsulated tarin on the cell cycle profile of U-87 MG cells over 48 h. Cells were challenged for 24 h or 48 h with free or nano-encapsulated tarin (both at 160 μg/mL), TMZ (33 μg/mL) or etoposide (2 mm), followed by PI staining and cell evaluation at every cycle phase by flow cytometry. The percentage of cells in the G0/G1 (dark blue), S (pink) and G2/M(green) phases are presented in bars on the left panel and representative histograms are shown in the right panel. * Indicates significant results compared to control cells, considering p <0.05.

a reduction in cells in the G0/G1 and S phases, reinforcing cell cycle arrest in the G2/M phase (Figure 6, bottom panel). This contrasts with what was observed in our previous study for a breast adenocarcinoma cell line (MDA-MB-231) in which cell cycle arrest also occurred, but in the G0/G1 phase.[42] No cell cycle changes were detected after exposing U-87 MG cells to free tarin (Figure 6, upper panel). TMZ caused a discrete accumulation of cells in the G0/G1 phase at both time points (Figure 6, upper panel). These data indicate that the U-87 MG cell growth and proliferation inhibition previously reported by our group may result from cell cycle arrest, avoiding mitosis conclusion in human glioma cell lines.[40,42]

Evaluation of Nano-Encapsulated Tarin Permeability to the Blood-Brain Barrier

To assess the ability of nano-encapsulated tarin to cross the blood-brain barrier, an in vitro BBB model was developed using a human brain microvascular endothelial cell line (hCMEC/D3) (Figure 7A and B and Table 1). A confluent cell monolayer was prepared and its transendothelial electrical resistance (TEER) was monitored periodically until reaching 64 Ωcm^{-2} (12 days), as reported previously.[51] Nano-encapsulated tarin (160 μg/mL) was then added to the culture medium and permeability was assessed over 180 min. In addition to TEER, monolayer permeability was monitored using lucifer yellow to ensure that the monolayer formed tight junctions. The nano-encapsulated tarin displayed a higher permeability coefficient (Pe) through the BBB model (8.66×10^{-3} cm/min) compared to lucifer yellow (2.98×10^{-3} cm/min), as lipophilic molecules are able to cross the hCMEC/D3 monolayers to a much greater extent than hydrophilic
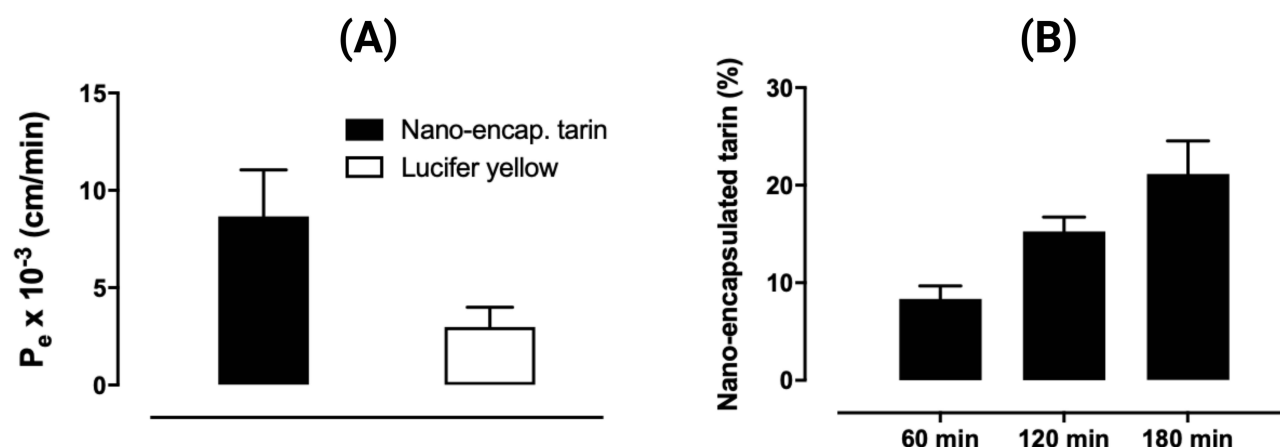
Figure 7 Transendothelial permeability of nano-encapsulated tarin. An in vitro blood-brain barrier was constructed using hCMEC/D3 cells and the transport of nano-encapsulated tarin was monitored over 180 min to determine the permeability coefficient (Pe) (**A**) and percentage of nano-encapsulated tarin recovered in the bottom chamber of the transwell plate (**B**). All experiments were conducted in triplicate.

ones[82] (Figure 7A and Table 1). Lucifer yellow was used as a permeability indicator and, although slightly higher permeability was noted compared to those reported by Markoutsa, Pampalakis, Niarakis, Romero, Weksler, Couraud, Antimisiaris,[51] the data confirmed an adequate barrier for the analyses. Concerning the nano-encapsulated tarin, the transport rate or permeability-surface area product (PS) over time was 4.07×10^{-3} mL/min, corresponding to a gradual accumulation in the bottom chamber, reaching 20% at 180 min (Figure 7B and Table 1). Transport rates for daunorubicin-loaded liposomes ranging from 8.47% to 24.91% in 24 h were described by Ying, Wen, Lu, Du, Guo, Tian, Men, Zhang, Li, Yang,[83] who observed increased transport when liposomes were functionalized with p-aminophenyl-α-D-manno-pyranoside and transferrin. Liposome functionalization/modification by the inclusion of macromolecules such as peptides, antibodies and polymers, can improve drug transport across the BBB.[29] The transport of nano-encapsulated tarin across the BBB model can, thus, be enhanced by nanocapsule liposome functionalization.

Therefore, considering that the hCMEC/D3 line is a well-characterized human endothelial brain cell line that gives rise to a BBB model, exhibiting all the characteristics required for good predictive transendothelial permeability and mimicking most of the basic physiological BBB characteristics,[82,84] the results indicate that nano-encapsulated tarin can overcome the BBB and reach targeted cancer cells, activating the molecular antitumoral response mechanisms reported herein.

In addition, it is important to note that, in our previous study, similar antitumoral mechanism patterns were observed for nano-encapsulated tarin against the MDA-MB-231 breast adenocarcinoma line.[42] Mitochondrial swelling, ER stress, cell cycle arrest, cell migration inhibition, caspase 3/7 activation, autophagosome formation and apoptosis activation were all part of both carcinoma cellular responses to nano-encapsulated tarin, indicating that nano-encapsulated tarin demonstrates a mode of action that follows a consistent pathway (Figure 8).

Moreover, other plant lectins have also been successfully tested in different human-derived glioma cell lineages (U-87 MG, GBM-1, SF-295). The mechanisms by which these lectins exert their effects on these cells are similar to those observed in the present study, including the induction of autophagic and apoptotic processes, activation of caspases 3–7

Table 1 Permeabillity Coefficient (Pe) and Permeability-Surface Area Product (PS)

Sample	PS x 10^{-3} (mL/min)	Pe x 10^{-3} (cm/min)
Nano-encapsulated tarin	4.07 ± 1.9	8.66 ± 4.1
Lucifer yellow	1.61 ± 0.6	2.98 ± 1.2

Abbreviations: PS, Permeability-surface area product; Pe, Permeability coefficient.
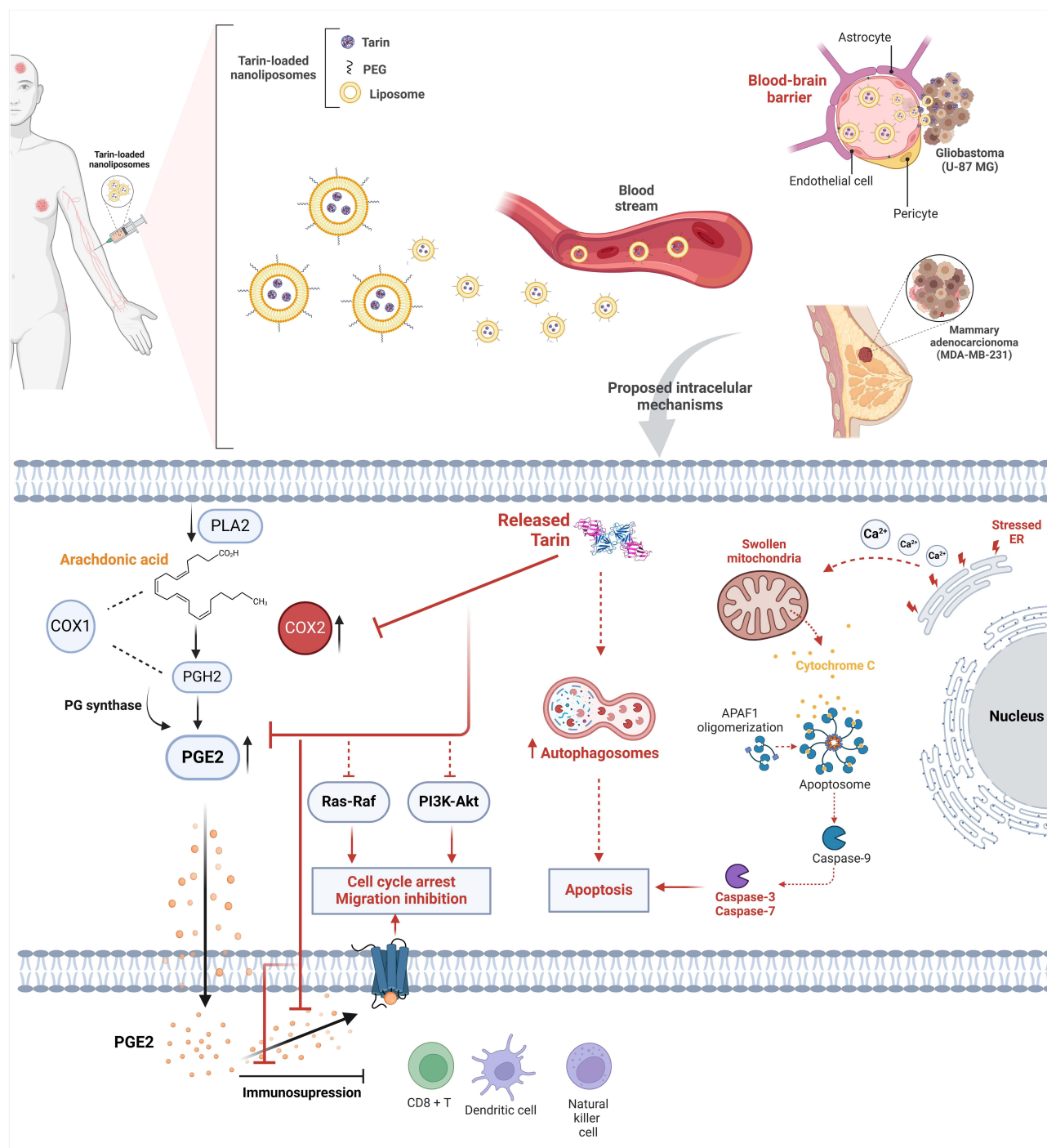
Figure 8 Proposed intracellular mechanisms triggered following the systemic administration of nano-encapsulated tarin in human glioblastoma and breast carcinoma lines. Tarin released from nanoliposomes activates intracellular signalization resulting in cell death by apoptosis by yet unraveled mechanisms. Red lines with line ends indicate previously reported tarin mechanisms, including reduced COX2 gene expression and a consequent decrease in the PGE2-mediated inflammatory response. Dashed red arrows indicate mechanisms already described for GNA-related lectins, but not yet proven for nano-encapsulated tarin. Red text includes the cancer cell effects described herein following treatment with nano-encapsulated tarin, comprising mitochondrial swelling, ER stress, cell cycle arrest, cell migration inhibition, caspase 3/7 activation, autophagosome formation and apoptosis activation. The proposed molecular mechanisms can be applied for both U-87 MG and MDA-MB-231 cells following treatment with nano-encapsulated tarin.

and cell cycle arrest.[85] The lectin isolated from *Abelmoschus esculentus* (AEL) potentiates ROS-induced apoptotic cell death mediated by caspases 3 and 7 in U-87 MG glioma cells, also promoting cell cycle arrest in the G0/G1 phases and inhibiting cell migration.[86] Autophagic cell death in U-87 MG cells, also detected by acridine orange staining, was observed for the lectin obtained from *Dioclea violacea* (DVL), attributed to a probable dephosphorylation of Akt-

mTORC1 pathway and consequent signaling suppression. Furthermore, this lectin was able to inhibit the migration and proliferation of U-87 MG glioma cells,[87] which was also observed in our studies. Considering the specific interaction between plant lectins and carbohydrates, several glycan targets were suggested as being involved in the antitumoral activity of plant lectins against glioma lineages, including matrix metalloproteinases, Epidermal Growth Factor Receptor (EGFR), CD98hc, AMPA Receptor, soluble form of CD73.[85] These molecules can provide abundant high N- and O-glycosylation targets connected to intracellular signaling involved in cell death through apoptosis and autophagy processes. *Galanthus nivalis* agglutinin, which belongs to the same family than tarin, can bind with high affinity to the soluble form of human CD73, which contributes to tumor progression and immunosuppression.[85,88]

Aberrant glycosylation patterns are a common event associated with tumorigenesis, playing critical roles in tumor progression, aggressiveness and therapeutic resistance.[89] In a previous study by our group, tarin was shown to bind to high affinity to high-mannose N-glycans and complex N-glycans, including paucimmanose, Lewis^Y epitope and antigen H2, which are abundantly present on the surface and in the intracellular compartment of cancerous cells.[37] Interestingly, paucimannosidic glycoepitopes have been proposed as a GBM biomarker. This epitope has been detected in high levels in aggressive human glioma U-87 MG cells and in a less aggressive line, U-138 MG, where it was proven to be involved in the negative control of cell proliferation, migration and invasion. The treatment of these cells with Manitou, an antibody that specifically binds paucimmannose, triggered decreases in cell proliferation, migration, invasion and adhesion, alongside the increase of paucimannose expression in both lines. It is believed that specific Manitou binding may activate unknown intracellular signaling that culminates in paucimannose upregulation and a consequent antitumoral response.[90] Interestingly, our previous study demonstrated that tarin can bind with higher affinity to fucosylated paucimannose, which is also present in U-87 MG cells and was associated with tumor progression in lung cancer.[46] Hence, it is possible that the tarin effects observed herein could be a result of the specific interaction with paucimannose glycoepitopes, but further studies should be conducted to investigate this hypothesis.

Conclusion

The results reported herein indicate that tarin, the lectin purified from taro (*Colocasia esculenta*), exhibits notable anti-cancer and anti-metastatic properties against glioblastoma cells, one of the most aggressive and invasive CNS tumors. Nano-encapsulated tarin administration at 160 µg/mL for up to 48 h to U-87 MG cells demonstrated significant efficacy in inducing apoptosis, as evidenced by the presence of apoptotic cells and caspase 3/7 activation. Furthermore, nano-encapsulated tarin disrupted cell regulation in the G2/M cell cycle phase and delayed tumor cell migration. Autophagy induction was also observed in U-87 MG cells, characterized by the presence of autophagosomes and ultrastructural changes, such as mitochondrial swelling. The efficiency of nano-encapsulated tarin crossing the BBB was demonstrated using the hCMEC/D3 endothelial cell line, a BBB model. Altogether, the results highlight nano-encapsulated tarin as a promising candidate for oncotherapy and eligible for systemic administration against glioblastomas, justifying future investigations, including cell uptake assay and proteomic analyses, to elucidate underlying molecular mechanisms, as well as animal model studies to evaluate the efficacy and safety of nano-encapsulated tarin. Moreover, the effect of nanoliposome-loaded tarin should be explored in animal models presenting tarin-sensitive tumors, as indicated by the presence of epitopes in tumoral cells that enable tarin recognition. This would provide deeper insights into the dual mechanisms triggered by tarin when protected by liposomal encapsulation. Experimental evidence suggests that, in vivo, tarin simultaneously inhibits cell carcinoma proliferation while enhancing the immune response against cancer, supporting ancient claims of taro's use in treating various diseases, which may not be associated to a single molecular mechanism.

Author Contributions

All authors made significant contributions to this study reported, whether study conception, design, execution, data acquisition, analysis and interpretation, or in all these areas; took part in drafting, revising or critically reviewing the article; gave final approval of the version to be published; have agreed on the journal to which the article has been submitted; and agree to be accountable for all aspects of the work.

Funding

Disclosure

The authors report no conflicts of interest in this work.

References

1. Claus EB, Walsh KM, Wiencke JK, et al. Survival and low-grade glioma: the emergence of genetic information. *Neurosurg Focus*. 2015;38(1):E6. doi:10.3171/2014.10.FOCUS12367
2. Uddin MS, Al Mamun A, Alghamdi BS, et al. Epigenetics of glioblastoma multiforme: from molecular mechanisms to therapeutic approaches. Paper presented at: Seminars in cancer biology. 2022.
3. Lathia JD, Mack SC, Mulkearns-Hubert EE, Valentim CL, Rich JN. Cancer stem cells in glioblastoma. *Genes Dev*. 2015;29(12):1203–1217. doi:10.1101/gad.261982.115
4. Gimple RC, Bhargava S, Dixit D, Rich JN. Glioblastoma stem cells: lessons from the tumor hierarchy in a lethal cancer. *Genes Dev*. 2019;33 (11–12):591–609. doi:10.1101/gad.324301.119
5. Ohgaki H, Kleihues P. Genetic pathways to primary and secondary glioblastoma. *Am J Pathol*. 2007;170(5):1445–1453. doi:10.2353/ajpath.2007.070011
6. Zong H, Parada LF, Baker SJ. Cell of origin for malignant gliomas and its implication in therapeutic development. *Cold Spring Harbor Perspect Biol*. 2015;7(5):a020610. doi:10.1101/cshperspect.a020610
7. Liebelt BD, Shingu T, Zhou X, Ren J, Shin SA, Hu J. Glioma stem cells: signaling, microenvironment, and therapy. *Stem Cells Inter*. 2016;2016(1). doi:10.1155/2016/7849890
8. Colwell N, Larion M, Giles AJ, et al. Hypoxia in the glioblastoma microenvironment: shaping the phenotype of cancer stem-like cells. *Neuro-Oncol*. 2017;19(7):887–896. doi:10.1093/neuonc/now258
9. Gabler L, Jaunecker CN, Katz S, et al. Fibroblast growth factor receptor 4 promotes glioblastoma progression: a central role of integrin-mediated cell invasiveness. *Acta Neuropathol Commun*. 2022;10(1):65. doi:10.1186/s40478-022-01363-2
10. Yabo YA, Niclou SP, Golebiewska A. Cancer cell heterogeneity and plasticity: a paradigm shift in glioblastoma. *Neuro-Oncol*. 2022;24(5):669–682. doi:10.1093/neuonc/noab269
11. Bush NAO, Chang SM, Berger MS. Current and future strategies for treatment of glioma. *Neurosurgical Rev*. 2017;40(1):1–14. doi:10.1007/s10143-016-0709-8
12. Gao H. Perspectives on dual targeting delivery systems for brain tumors. *J Neuroimmune Pharmacol*. 2017;12(1):6–16. doi:10.1007/s11481-016-9687-4
13. Vanza J, Jani P, Pandya N, Tandel H. Formulation and statistical optimization of intravenous temozolomide-loaded PEGylated liposomes to treat glioblastoma multiforme by three-level factorial design. *Drug De Ind Pharm*. 2018;44(6):923–933. doi:10.1080/03639045.2017.1421661
14. Jo J, Schiff D. Current considerations in the treatment of grade 3 gliomas. *Curr Treat Opt Oncol*. 2022;23(9):1219–1232. doi:10.1007/s11864-022-01000-z
15. Zhao M, van Straten D, Broekman ML, Préat V, Schiffelers RM. Nanocarrier-based drug combination therapy for glioblastoma. *Theranostics*. 2020;10(3):1355. doi:10.7150/thno.38147
16. Safa AR, Saadatzadeh MR, Cohen-Gadol AA, Pollok KE, Bijangi-Vishehsaraei K. Glioblastoma stem cells (GSCs) epigenetic plasticity and interconversion between differentiated non-GSCs and GSCs. *Genes Dis*. 2015;2(2):152–163. doi:10.1016/j.gendis.2015.02.001
17. Zhang J, Stevens M FG, Bradshaw T D. Temozolomide: mechanisms of action, repair and resistance. *Current Molecular Pharmacol*. 2012;5 (1):102–114. doi:10.2174/1874467211205010102
18. Gao J, Wang Z, Liu H, Wang L, Huang G. Liposome encapsulated of temozolomide for the treatment of glioma tumor: preparation, characterization and evaluation. *Drug Dis Ther*. 2015;9(3):205–212. doi:10.5582/ddt.2015.01016
19. Afzalipour R, Khoei S, Khoee S, et al. Dual-targeting temozolomide loaded in folate-conjugated magnetic triblock copolymer nanoparticles to improve the therapeutic efficiency of rat brain gliomas. *ACS Biomater Sci Eng*. 2019;5(11):6000–6011. doi:10.1021/acsbiomaterials.9b00856
20. Singh N, Miner A, Hennis L, Mittal S. Mechanisms of temozolomide resistance in glioblastoma-a comprehensive review. *Cancer Drug Resis*. 2021;4(1):17. doi:10.20517/cdr.2020.79
21. Champeaux C, Weller J. Implantation of carmustine wafers (Gliadel®) for high-grade glioma treatment. A 9-year nationwide retrospective study. *J Neuro-oncol*. 2020;147(1):159–169. doi:10.1007/s11060-020-03410-1
22. Ashby LS, Smith KA, Stea B. Gliadel wafer implantation combined with standard radiotherapy and concurrent followed by adjuvant temozolomide for treatment of newly diagnosed high-grade glioma: a systematic literature review. *World J Surg Oncol*. 2016;14(1):1–15. doi:10.1186/s12957-016-0975-5
23. Mittal S, Klinger NV, Michelhaugh SK, Barger GR, Pannullo SC, Juhász C. Alternating electric tumor treating fields for treatment of glioblastoma: rationale, preclinical, and clinical studies. *J Neurosurg*. 2017;128(2):414–421. doi:10.3171/2016.9.JNS16452
24. Kinzel A, Ambrogi M, Varshaver M, Kirson ED. Tumor treating fields for glioblastoma treatment: patient satisfaction and compliance with the second-generation Optune® system. *Clinl Med Insights Oncol*. 2019;13:1179554918825449. doi:10.1177/1179554918825449

25. Guberina N, Pöttgen C, Kebir S, et al. Combined radiotherapy and concurrent tumor treating fields (TTFields) for glioblastoma: dosimetric consequences on non-coplanar IMRT as initial results from a phase I trial. *Radiat Oncol.* 2020;15(1):1–11. doi:10.1186/s13014-020-01521-7

26. Stupp R, Taillibert S, Kanner A, et al. Effect of tumor-treating fields plus maintenance temozolomide vs maintenance temozolomide alone on survival in patients with glioblastoma: a randomized clinical trial. *JAMA.* 2017;318(23):2306–2316. doi:10.1001/jama.2017.18718

27. Ruan S, Zhou Y, Jiang X, Gao H. Rethinking CRITID procedure of brain targeting drug delivery: circulation, blood brain barrier recognition, intracellular transport, diseased cell targeting, internalization, and drug release. *Adv Sci.* 2021;8(9):2004025. doi:10.1002/advs.202004025

28. Cardoso RV, Pereira PR, Freitas CS, Paschoalin VMF. Trends in drug delivery systems for natural bioactive molecules to treat health disorders: the importance of nano-liposomes. *Pharmaceutics.* 2022;14(12):2808. doi:10.3390/pharmaceutics14122808

29. Vieira DB, Gamarra LF. Getting into the brain: liposome-based strategies for effective drug delivery across the blood–brain barrier. *Int J Nanomed.* 2016;Volume 11:5381–5414. doi:10.2147/IJN.S117210

30. Sanna V, Pala N, Sechi M. Targeted therapy using nanotechnology: focus on cancer. *Int J Nanomed.* 2014;9:467–483. doi:10.2147/IJN.S36654

31. Brandsma D, Kerklaan BM, Diéras V, et al. Phase 1/2a study of glutathione pegylated liposomal doxorubicin (2b3-101) in patients with brain metastases (BM) from solid tumors or recurrent high grade gliomas (HGG). *Ann Oncol.* 2014; 25:iv157.

32. Kasenda B, König D, Manni M, et al. Targeting immunoliposomes to EGFR-positive glioblastoma. *ESMO open.* 2022;7(1):100365. doi:10.1016/j.esmoop.2021.100365

33. Pepper JW, Scott Findlay C, Kassen R, Spencer SL, Maley CC. Synthesis: cancer research meets evolutionary biology. *Evol Appl.* 2009;2(1):62–70. doi:10.1111/j.1752-4571.2008.00063.x

34. Yagüe E, Arance A, Kubitza L, et al. Ability to acquire drug resistance arises early during the tumorigenesis process. *Cancer Res.* 2007;67(3):1130–1137. doi:10.1158/0008-5472.CAN-06-2574

35. Piwowarczyk L, Mlynarczyk DT, Krajka-Kuźniak V, et al. Natural compounds in liposomal nanoformulations of potential clinical application in glioblastoma. *Cancers.* 2022;14(24):6222. doi:10.3390/cancers14246222

36. Pereira PR, Del Aguila EM, Verícimo MA, Zingali RB, Paschoalin VMF, Silva JT. Purification and characterization of the lectin from taro (Colocasia esculenta) and its effect on mouse splenocyte proliferation in vitro and in vivo. *The Protein J.* 2014;33(1):92–99. doi:10.1007/s10930-013-9541-y

37. Pereira PR, Winter HC, Verícimo MA, et al. Structural analysis and binding properties of isoforms of tarin, the GNA-related lectin from Colocasia esculenta. *Biochimica et Biophysica Acta.* 2015;1854(1):20–30. doi:10.1016/j.bbapap.2014.10.013

38. Pereira PR, Meagher JL, Winter HC, et al. High-resolution crystal structures of Colocasia esculenta tarin lectin. *Glycobiology.* 2017;27(1):50–56. doi:10.1093/glycob/cww083

39. Mérida LA, Mattos ÉB, Corrêa AC, et al. Tarin stimulates granulocyte growth in bone marrow cell cultures and minimizes immunosuppression by cyclo-phosphamide in mice. *PLoS One.* 2018;13(11):e0206240. doi:10.1371/journal.pone.0206240

40. Corrêa AC, Vericimo MA, Dashevskiy A, Pereira PR, Paschoalin VM. Liposomal taro lectin nanocapsules control human glioblastoma and mammary adenocarcinoma cell proliferation. *Molecules.* 2019;24(3):471. doi:10.3390/molecules24030471

41. EBdA M, Pereira PR, Mérida LAD, et al. Taro lectin can act as a cytokine-mimetic compound, stimulating myeloid and T lymphocyte lineages and protecting progenitors in murine bone marrow. *Pharmaceutics.* 2021;13(3):350. doi:10.3390/pharmaceutics13030350

42. Cardoso RV, Pereira PR, Freitas CS, et al. Tarin-loaded nanoliposomes activate apoptosis and autophagy and inhibit the migration of human mammary adenocarcinoma cells. *Int J Nanomed.* 2023;18:6393–6408. doi:10.2147/IJN.S434626

43. Pereira PR, Acntf C, Vericimo MA, Paschoalin VMF. Tarin, a potential immunomodulator and COX-inhibitor lectin found in taro (Colocasia esculenta). *Compr Rev Food Sci Food Saf.* 2018;17(4):878–891. doi:10.1111/1541-4337.12358

44. Pereira PR, Silva JT, Verícimo MA, Paschoalin VM, Teixeira GA. Crude extract from taro (Colocasia esculenta) as a natural source of bioactive proteins able to stimulate haematopoietic cells in two murine models. *J Func Foods.* 2015;18:333–343. doi:10.1016/j.jff.2015.07.014

45. Corrêa AC, Pereira PR, Paschoalin VM. Preparation and characterization of nanoliposomes for the entrapment of bioactive hydrophilic globular proteins. *JoVE.* 2019;(150):e59900.

46. Jia L, Zhang J, Ma T, Guo Y, Yu Y, Cui J. The function of fucosylation in progression of lung cancer. *Front Oncol.* 2018;8:565. doi:10.3389/fonc.2018.00565

47. Pinho SS, Reis CA. Glycosylation in cancer: mechanisms and clinical implications. *Nat Rev Cancer.* 2015;15(9):540–555. doi:10.1038/nrc3982

48. Yau T, Dan X, Ng CCW, Ng TB. Lectins with potential for anti-cancer therapy. *Molecules.* 2015;20(3):3791–3810. doi:10.3390/molecules20033791

49. Vervecken W, Kleff S, Pfüller U, Büssing A. Induction of apoptosis by mistletoe lectin I and its subunits. No evidence for cytotoxic effects caused by isolated A-and B-chains. *Int J Biochem Cell Biol.* 2000;32(3):317–326. doi:10.1016/S1357-2725(99)00135-1

50. Roy A, Banerjee S, Majumder P, Das S. Efficiency of mannose-binding plant lectins in controlling a homopteran insect, the red cotton bug. *J AgriFood Chem.* 2002;50(23):6775–6779. doi:10.1021/jf025660x

51. Markoutsa E, Pampalakis G, Niarakis A, et al. Uptake and permeability studies of BBB-targeting immunoliposomes using the hCMEC/D3 cell line. *Eur J Pharm Biopharm.* 2011;77(2):265–274. doi:10.1016/j.ejpb.2010.11.015

52. Grada A, Otero-Vinas M, Prieto-Castrillo F, Obagi Z, Falanga V. Research techniques made simple: analysis of collective cell migration using the wound healing assay. *J Invest Dermatol.* 2017;137(2):e11–e16. doi:10.1016/j.jid.2016.11.020

53. Diniz Filho JFS, de Barros A, Pijeira MSO, et al. Ultrastructural analysis of cancer cells treated with the radiopharmaceutical radium dichloride ([223Ra] RaCl2): understanding the effect on cell structure. *Cells.* 2023;12(3):451. doi:10.3390/cells12030451

54. Thomé MP, Filippi-Chiela EC, Villodre ES, et al. Ratiometric analysis of acridine orange staining in the study of acidic organelles and autophagy. *J Cell Sci.* 2016;129(24):4622–4632. doi:10.1242/jcs.195057

55. W-l Y, Zhao Y-P, H-q L, et al. Doxorubicin-poly (ethylene glycol)-alendronate self-assembled micelles for targeted therapy of bone metastatic cancer. *Sci Rep.* 2015;5(1):14614. doi:10.1038/srep14614

56. Casella JF, Flanagan MD, Lin S. Cytochalasin D inhibits actin polymerization and induces depolymerization of actin filaments formed during platelet shape change. *Nature.* 1981;293(5830):302–305. doi:10.1038/293302a0

57. Shoji K, Ohashi K, Sampei K, Oikawa M, Mizuno K. Cytochalasin D acts as an inhibitor of the actin–cofilin interaction. *Biochem Biophys Res Commun.* 2012;424(1):52–57. doi:10.1016/j.bbrc.2012.06.063

58. Khiabani NA, Doustvandi MA, Mohammadnejad F, et al. Combination of B7H6-siRNA and temozolomide synergistically reduces stemness and migration properties of glioblastoma cancer cells. *Exp Cell Res*. 2023;429(1):113667. doi:10.1016/j.yexcr.2023.113667

59. Pekmez M, Kılcı C. The effect of temozolomide on Hsp60 and Hsp70 expression in extracellular vesicles derived from U87MG glioma cells. *Turk JBiochem*. 2022;47(1):85–95. doi:10.1515/tjb-2021-0111

60. Vengoji R, Macha MA, Nimmakayala RK, et al. Afatinib and Temozolomide combination inhibits tumorigenesis by targeting EGFRvIII-cMet signaling in glioblastoma cells. *J Exp Clin Cancer Res*. 2019;38:1–13. doi:10.1186/s13046-019-1264-2

61. Fares J, Fares MY, Khachfe HH, Salhab HA, Fares Y. Molecular principles of metastasis: a hallmark of cancer revisited. *Signal Transdu Targeted Therapy*. 2020;5(1):28. doi:10.1038/s41392-020-0134-x

62. J-s W, Jiang J, B-j C, Wang K, Y-l T, X-h L. Plasticity of cancer cell invasion: patterns and mechanisms. *Transl Oncol*. 2021;14(1):100899. doi:10.1016/j.tranon.2020.100899

63. Society AC. How targeted therapies are used to treat cancer. 2021. Available from: https://www.cancer.org/cancer/managing-cancer/treatment-types/targeted-therapy/what-is.html. Accessed 4, 2024.

64. Moustapha A, Pérétout P, Rainey N, et al. Curcumin induces crosstalk between autophagy and apoptosis mediated by calcium release from the endoplasmic reticulum, lysosomal destabilization and mitochondrial events. *Cell Death Discovery*. 2015;1(1):1–15. doi:10.1038/cddiscovery.2015.17

65. Jakubczyk K, Drużga A, Katarzyna J, Skonieczna-żydecka K. Antioxidant potential of curcumin-a meta-analysis of randomized clinical trials. *Antioxidants*. 2020;9(11):109.

66. Martucciello S, Masullo M, Cerulli A, Piacente S. Natural products targeting ER stress, and the functional link to mitochondria. *Int J mol Sci*. 2020;21(6):1905. doi:10.3390/ijms21061905

67. Varghese E, Samuel SM, Sadiq Z, et al. Anti-cancer agents in proliferation and cell death: the calcium connection. *Int J mol Sci*. 2019;20(12):3017. doi:10.3390/ijms20123017

68. Tilija Pun N, Jang W-J, Jeong C-H. Role of autophagy in regulation of cancer cell death/apoptosis during anti-cancer therapy: focus on autophagy flux blockade. *Arch Pharmacal Res*. 2020;43(5):475–488. doi:10.1007/s12272-020-01239-w

69. Das S, Shukla N, Singh SS, Kushwaha S, Shrivastava R. Mechanism of interaction between autophagy and apoptosis in cancer. *Apoptosis*. 2021;26(9):512–533. doi:10.1007/s10495-021-01687-9

70. Liu Z, Luo Y, Zhou TT, Zhang WZ. Could plant lectins become promising anti-tumour drugs for causing autophagic cell death? *Cell Proliferation*. 2013;46(5):509–515. doi:10.1111/cpr.12054

71. Wu L, J-k B. Anti-tumor and anti-viral activities of Galanthus nivalis agglutinin (GNA)-related lectins. *Glycoconjugate Journal*. 2013;30(3):269–279. doi:10.1007/s10719-012-9440-z

72. C-y L, Meng L, Liu B, J-k B. Galanthus nivalis agglutinin (GNA)-related lectins: traditional proteins, burgeoning drugs? *Current Chem Biol*. 2009;3(3):323–333. doi:10.2174/187231309789054913

73. Bhutia SK, Panda PK, Sinha N, et al. Plant lectins in cancer therapeutics: targeting apoptosis and autophagy-dependent cell death. *Pharmacol Res*. 2019;144:8–18. doi:10.1016/j.phrs.2019.04.001

74. Kwantwi LB. The dual role of autophagy in the regulation of cancer treatment. *Amino Acids*. 2024;56(1):7. doi:10.1007/s00726-023-03364-4

75. Maes H, Rubio N, Garg AD, Agostinis P. Autophagy: shaping the tumor microenvironment and therapeutic response. *Trends Mol Med*. 2013;19(7):428–446. doi:10.1016/j.molmed.2013.04.005

76. Boehning D, Patterson RL, Sedaghat L, Glebova NO, Kurosaki T, Snyder SH. Cytochrome c binds to inositol (1, 4, 5) trisphosphate receptors, amplifying calcium-dependent apoptosis. *Nat Cell Biol*. 2003;5(12):1051–1061. doi:10.1038/ncb1063

77. Lee JK, Lu S, Madhukar A. Real-time dynamics of Ca2+, caspase-3/7, and morphological changes in retinal ganglion cell apoptosis under elevated pressure. *PLoS One*. 2010;5(10):e13437. doi:10.1371/journal.pone.0013437

78. Chavda VP, Patel AB, Mistry KJ, et al. Nano-drug delivery systems entrapping natural bioactive compounds for cancer: recent progress and future challenges. *Front Oncol*. 2022;12:867655. doi:10.3389/fonc.2022.867655

79. Hegde M, Girisa S, BharathwajChetty B, Vishwa R, Kunnumakkara AB. Curcumin formulations for better bioavailability: what we learned from clinical trials thus far? *ACS omega*. 2023;8(12):10713–10746. doi:10.1021/acsomega.2c07326

80. Schonn I, Hennesen J, Dartsch DC. Cellular responses to etoposide: cell death despite cell cycle arrest and repair of DNA damage. *Apoptosis*. 2010;15(2):162–172. doi:10.1007/s10495-009-0440-9

81. Montecucco A, Zanetta F, Biamonti G. Molecular mechanisms of etoposide. *EXCLI J*. 2015;14:95–108. doi:10.17179/excli2015-561

82. Poller B, Gutmann H, Krähenbühl S, et al. The human brain endothelial cell line hCMEC/D3 as a human blood-brain barrier model for drug transport studies. *J Neurochem*. 2008;107(5):1358–1368.

83. Ying X, Wen H, Lu W-L, et al. Dual-targeting daunorubicin liposomes improve the therapeutic efficacy of brain glioma in animals. *J Control Release*. 2010;141(2):183–192. doi:10.1016/j.jconrel.2009.09.020

84. Weksler B, Subileau E, Perriere N, et al. Blood-brain barrier-specific properties of a human adult brain endothelial cell line. *FASEB J*. 2005;19(13):1872–1874. doi:10.1096/fj.04-3458fje

85. Leal RB, Pinto-Junior VR, Oliveira MV, et al. The antiglioma potential of plant lectins: molecular targets, mechanisms, and future directions. *Neuroglia*. 2025;6(1):5. doi:10.3390/neuroglia6010005

86. Musthafa SA, Muthu K, Vijayakumar S, et al. Lectin isolated from Abelmoschus esculentus induces caspase mediated apoptosis in human U87 glioblastoma cell lines and modulates the expression of circadian clock genes. *Toxicon*. 2021;202:98–109. doi:10.1016/j.toxicon.2021.08.025

87. Nascimento APM, Wolin IAV, Welter PG, et al. Lectin from Dioclea violacea induces autophagy in U87 glioma cells. *Int J Biol Macromol*. 2019;134:660–672. doi:10.1016/j.ijbiomac.2019.04.203

88. Heuts DPHM, Weissenborn MJ, Olkhov RV, et al. Crystal structure of a soluble form of human CD73 with ecto-5′-nucleotidase activity. *ChemBioChem*. 2012;13(16):2384–2391. doi:10.1002/cbic.201200426

89. Thomas D, Rathinavel AK, Radhakrishnan P. Altered glycosylation in cancer: a promising target for biomarkers and therapeutics. *Biochim Biophys Acta Rev Cancer*. 2021;1875(1):188464. doi:10.1016/j.bbcan.2020.188464

90. Becker Y, Förster S, Gielen GH, et al. Paucimannosidic glycoepitopes inhibit tumorigenic processes in glioblastoma multiforme. *Oncotarget*. 2019;10(43):4449–4465. doi:10.18632/oncotarget.27056